High-precision nuclear beta decay half-life measurement of $^{26}Al^{m}$ by a digital beta counting method

L. Chen, J. C. Hardy, M. Bencomo, V. Horvat, N. Nica, and H. I. Park

We have been developing a digital β-counting system over the past few years. Its principle and some preliminary test results were reported in last year's progress report [1]. In 2012-13 we have finished the data analysis of an on-line experiment in which the digital counting method was used to measure the $^{26}Al^{m}$ half-life. A detailed paper has been submitted recently for publication in Nuclear Instruments and Methods [2]. Here we report some details of the data analysis and the results of our on-line measurement of the $^{26}Al^{m}$ half-life.

By using pulse-shape analysis, we can now clearly distinguish a true β signal from a spurious one. Since we also record the time of arrival of each pulse, we have been able to examine time correlations between the two types of events. The measured time separation between successive events is plotted in Fig. 1, where the two panels illustrate the same data but are displayed with different time scales.

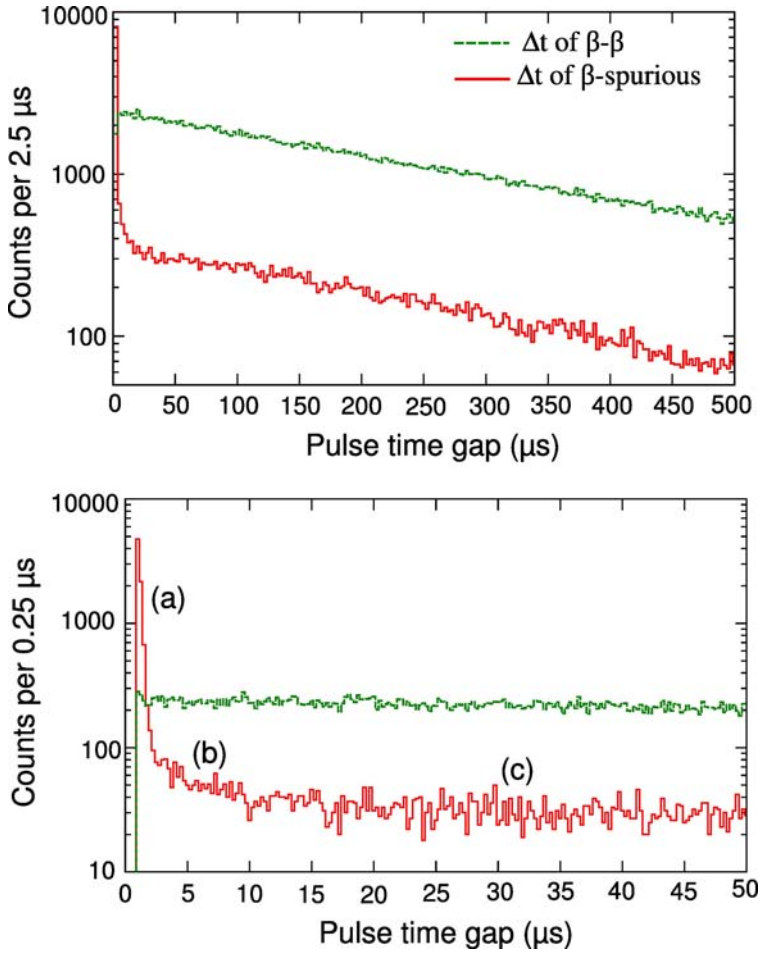

FIG. 1. The top panel plots the time-gap distribution of pulses over a period of 500 μs, measured with a 3 kBq β source at a detector bias of 2700 V. The bottom panel shows a zoomed-in plot of the same data to show the short-time details of the distribution.

The histograms identified as “β-β” give the distribution of time-gaps between two identified β's. The histograms identified as “β-spurious" give the distribution of time gaps that begin with an identified β event and end with a spurious pulse. In the bottom panel, the β-spurious histogram exhibits three different slopes, which are denoted as (a), (b) and (c). The first two correspond to fast spurious signals which appear within ~1 μs and ~10 μs, respectively, after a β signal. The third has a slope very similar to that of the β-β histogram. The results in Fig. 1 demonstrate that some spurious pulses are tightly time-correlated with a particular β signal: the events in the first 10 μs that contribute to the part of the histogram with slopes (a) and (b). However, the spurious events that constitute the remainder of the β-spurious plot, with slope (c), are probably not -- at least not within the time scale to which we are sensitive. Slope (c) is identical to the slope of the β-β histogram and reflects the fact that, after a β event has “started the clock", the appearance of a second β stops the clock, thus eliminating the possibility of a β-spurious correlation being recorded.

To characterize the performance of our digital counting system, we performed an on-line test experiment to measure the 6.345-s half-life of the superallowed β^+ emitter $^{26}Al^m$. The half-life of $^{26}Al^m$ has been measured before by a number of groups with consistent results [3,4,5] so it can serve as a good standard for test purposes.

The on-line measurement dead time for each event was 800 ns. To correct for lost events we followed the shadow window technique, which was introduced by Lynch in a recent measurement of the muon half-life [6]. This technique, schematically illustrated in Fig. 2, is a statistically correct method, which is also independent of the counting rate. After each recorded event, real or spurious, there is a dead-time during which real β events might be missed. We determine the possible loss for each event by placing a time-window with the same length as the dead-time at some predetermined time later (or earlier) in the same cycle. If the time between the observed event and this shadow window is much shorter than the decay half-life being measured, then the contents of the shadow window accurately reflect the loss due to the original dead-time. If the shadow window includes an event, then it too is partially dead and a second (shorter) shadow window to account for its dead time must be applied after a second delay. This process continues until no event is observed in the shadow window.

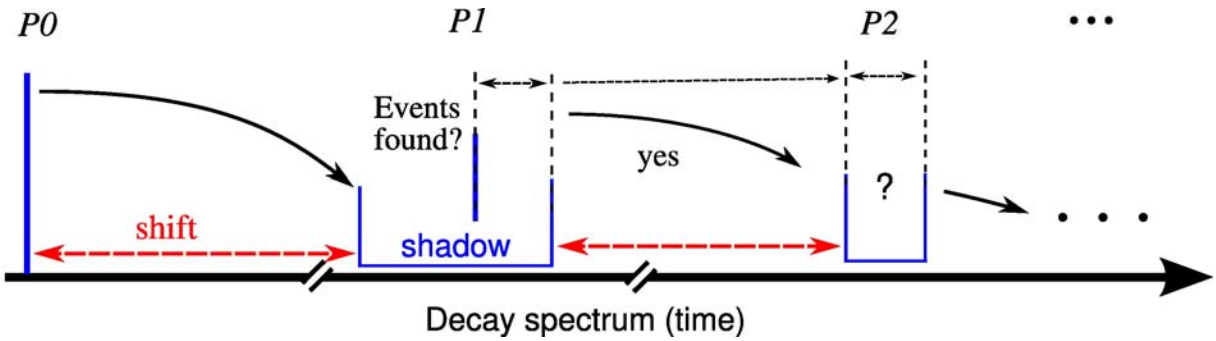

FIG. 2. A schematic illustration of the shadow window technique used to correct for dead time. P0 is the original pulse and P1 and P2 are events that may appear (or may not) in the first and second-order shadow window, respectively. The first order shadow window has the same length as that of the system dead time. The second-order window, if required, has a length equal to the part of the first-order window that is made dead by the appearance of P1. The process continues to a third-order window if P2 occurs, and so on.

In principle, to be reliable this method requires only that the delay time between the event and the shadow window be much shorter than the decay half-life; in reality, we found that the shadow window cannot be placed too near the original pulse on the down-stream side since there is a significant probability of a correlated β-spurious pair of events within a few hundred μs of one another (see Fig.1). We chose to avoid this problem by placing the shadow window 10 ms later than the original pulse to totally avoid this problem. That is corresponding to a 0.16% shift in terms of the half-life of $^{26}Al^{m}$. And in our analysis, we got consistent results when the shadow window was placed 50 μs in the up-stream side or 5 ms in the down-stream side.

After dead-time corrections had been made, we built a decay spectrum for each tape cycle. We then used the same fitting procedure as described in our previous papers (for example, Ref.[7]). We also artificially introduced into our software analysis a dead time after each event, which was significantly longer than the system's inherent 800 ns dead time. This way the software could also examine if any events appeared near the end of the imposed dead time and increase the shadow length in that case to incorporate the component of the inherent dead time that extended beyond the end of the imposed one. We reanalyzed our data a number of times with imposed dead times that ranged from 2 μs to 12 μs. The result is plotted in Fig. 3. The result we ultimately quote is from the analysis with an imposed dead time of 4 μs.

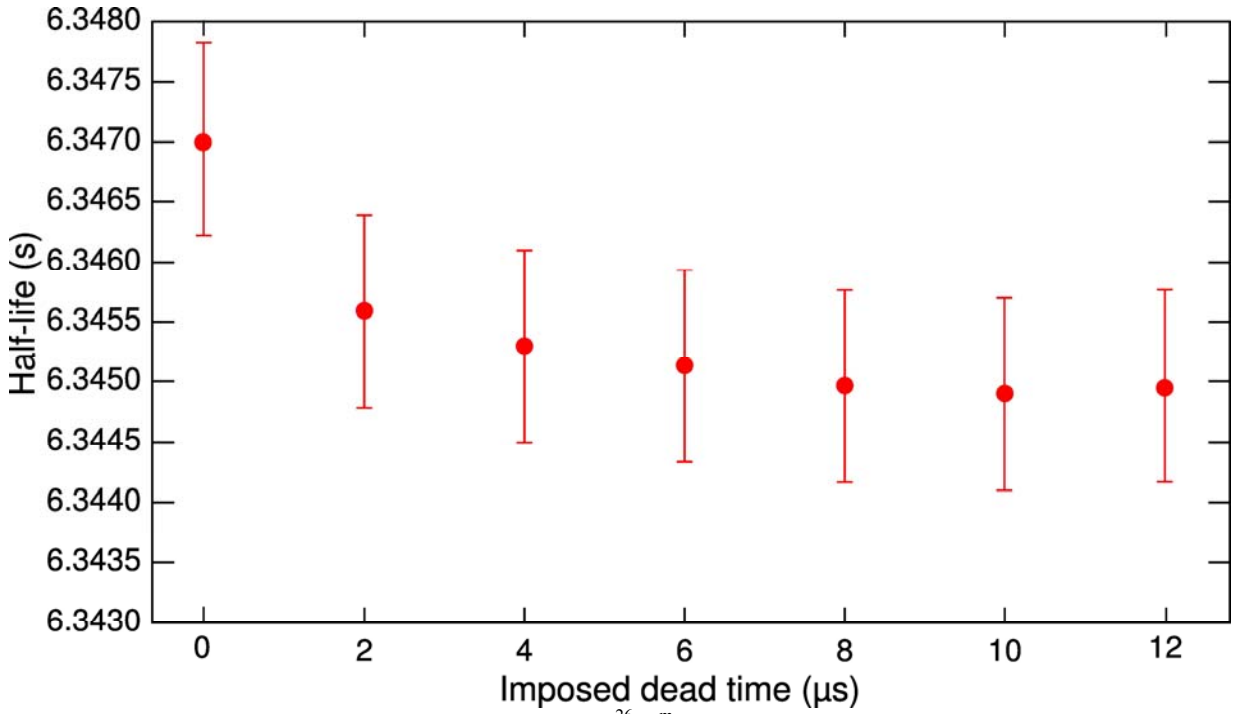

FIG. 3. Half lives obtained from the measured decay of $^{26}Al^{m}$ plotted as a function of the imposed dead time used in analysis. Note that the total dead time is equal to the imposed dead time or the inherent system dead time (800 ns), whichever is greater.

All spectra were fitted with the ROOT Minute2 package using the Maximum Likelihood method. Our fitting code was also tested with Monte Carlo generated decay data, in which there were 10^{9} events

with a decay half-life set to 6.34500 s. The half-life we obtained from fitting the simulated data was 6.34502(25) s, which successfully confirmed our fitting routines.

The evaluated half-lives of the 14 runs taken with 2650, 2700 and 2750 V detector bias are plotted in Fig. 4. Four runs with 2800 V bias, which is just above the plateau region, had significantly more spurious events and their overall analysis was not as satisfactory as it was for the other runs with lower bias voltages well within the plateau region, so we decided to eliminate them entirely. The average value of the results in Fig. 4 is 6345.30±0.90 ms.

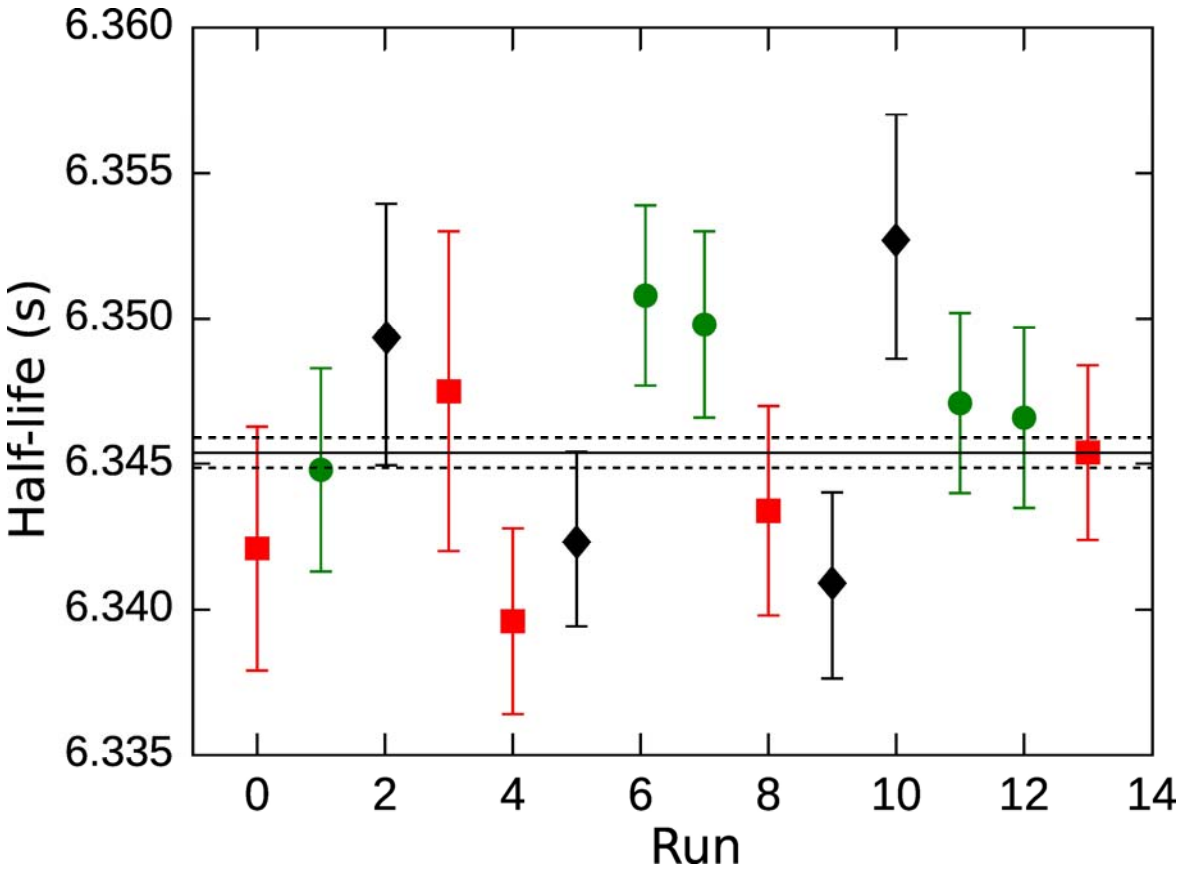

FIG. 4. The evaluated half-lives of 14 runs. The runs with bias 2650 V, 2700 V, 2750 V are represented by diamond, square, and circle, respectively.

In Fig. 5 we regroup the individual cycles according to their initial β-decay counting rate and obtain a half-life from each group. It is gratifying to see that there is no systematic dependence of the measured half-life on the experimental counting rate. All potential impurities identified at the MARS focal plane are stable isotopes so there is no need to incorporate any systematic uncertainty to our $^{26}Al^{m}$ half-life result to account for sample impurities. We therefore quote our final result for the $^{26}Al^{m}$ half-life to be 6345.30±0.90 ms, where the uncertainty is determined by counting statistics alone. This result is consistent with the 2009 published world average, 6345.0±1.9 ms [3], but has twice the precision. Our result also agrees with two measurements that have been published since 2009: 6346.54±0.46(stat)±0.60(syst) ms [4] and 6347.8±2.5 ms [5].

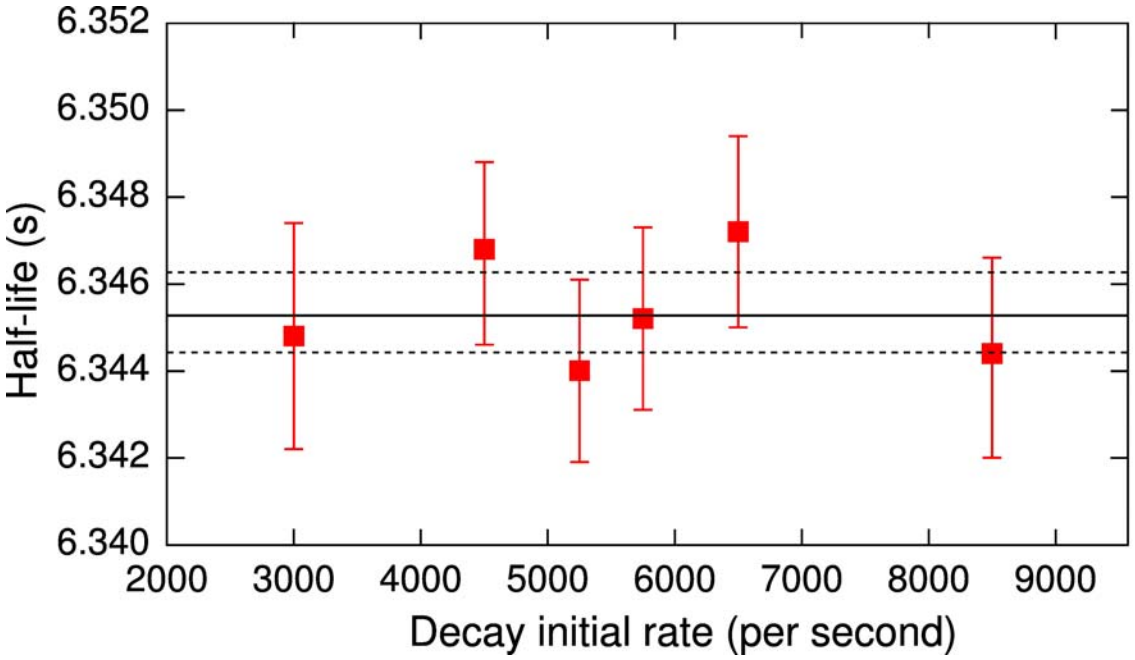

FIG. 5. The evaluated half-lives of as a function of initial decay rates. Cycles are regrouped in 6 groups according to their initial decay rate (in thousand per second): (2-4), (4-5), (5-5.5), (5.5-6), (6-7) and (7-10). The ranges for each group were chosen to include approximately equal numbers of events. The half-life results are plotted at the mid-point of each range.

[1] L. Chen and J.C. Hardy, *Progress in Research*, Cyclotron Institute, Texas A&M University (2011-2012), p. V-24.

[2] L. Chen, J C. Hardy, M. Bencomo, V. Horvat, N. Nica, and H.I. Park, Nucl, Instrum. Methods. Phys. Res. A. (submitted).

[3] J.C. Hardy and I.S. Towner, Phys. Rev. C **79**, 055502 (2009).

[4] P. Finlay, S. Ettenauer, G.C. Ball *et al.*, Phys. Rev. Lett. **106**, 032501 (2011).

[5] R.J. Scott, G.J. O'Keefe, M.N. Thompson and R.P. Rassool, Phys. Rev. C **84**, 024611 (2011).

[6] Kevin R. Lynch, Nucl. Phys. **B189**, 15 (2009).

[7] E. Iacob, J.C. Hardy *et al.*, Phys. Rev. C **82**, 035502 (2010).